Please cite as:

Arroo RRJ, Sari S, Barut B, Özel A, Ruparelia KC, Şöhretoğlu D (2020) Flavones as tyrosinase inhibitors: kinetic studies *in vitro* and *in silico*. Phytochem Anal. 31(3): 314-321. https://doi.org/10.1002/pca.2897

Epub 2020 Jan 29

Flavones as tyrosinase inhibitors: kinetic studies *in vitro* and *in silico*

Randolph RJ Arroo[a, *], Suat Sari[b], Burak Barut[c], Arzu Özel[c,d], Ketan C Ruparelia[a], Didem Şöhretoğlu[e]

[a*] Leicester School of Pharmacy, De Montfort University, The Gateway, Leicester LE1 9BH, United Kingdom

[b]Hacettepe University, Faculty of Pharmacy, Department of Pharmaceutical Chemistry, Sıhhiye, Ankara, TR-06100, Ankara, Turkey

[c]Karadeniz Technical University, Faculty of Pharmacy, Department of Biochemistry, Trabzon,Turkey

[d]Karadeniz Technical University, Drug and Pharmaceutical Technology Application and Research Center, Trabzon, Turkey

[e]Hacettepe University, Faculty of Pharmacy, Department of Pharmacognosy, Sıhhiye, Ankara, TR-06100, Ankara, Turkey

* Corresponding author:

Leicester School of Pharmacy, De Montfort University, The Gateway

Leicester LE1 9BH, United Kingdom

E-mail: rrjarroo@dmu.ac.uk

Tel: +44 116 250 6386

Abstract

Introduction – Tyrosinase is a multifunctional copper-containing oxidase enzyme that catalyzes the first steps in the formation of melanin pigments. Identification of tyrosinase inhibitors is of value for applications in cosmetics, medicine and agriculture.

Objective – To develop an analytical method that allows identification of drug-like natural products that can be further developed as tyrosinase inhibitors. Results of in vitro and in silico studies will be compared in order to gain a deeper insight into the mechanism of action of enzyme inhibition.

Method – Using an in vitro assay we tested tyrosinase inhibitor effects of five structurally related flavones, i.e. luteolin (**1**), eupafolin (**2**), genkwanin (**3**), nobiletin (**4**), and chrysosplenetin (**5**). The strongest inhibitors were further investigated in silico, using enzyme docking simulations.

Results - All compounds tested showed modest tyrosinase inhibitory effect compared to the positive control, kojic acid. The polymethoxy flavones **4** and **5** exhibited the strongest tyrosinase inhibitory effect with IC_{50} values of 131.92 ± 1.75 μM and 99.87 ± 2.38 μM respectively. According to kinetic analysis **2**, **4** and **5** were competitive inhibitors, whereas **1** and **3** were noncompetitive inhibitors of tyrosinase. Docking studies indicated that methoxy groups on **4** and **5** caused steric hindrance which prevented alternative binding modes in the tyrosinase; the methoxy groups on the B-ring of these flavones faced the catalytic site in the enzyme.

Conclusions – The docking simulations nicely complemented the in vitro kinetic studies, opening the way for the development of predictive models for use in drug design.

Key words - Flavonoid; tyrosinase; enzyme kinetics; molecular docking

1. INTRODUCTION

Tyrosinase is a multifunctional copper-containing oxidase enzyme that is pivotal for the production of melanin pigments in bacteria, fungi, plants, and mammals (Chen et al., 2016; Gou et al., 2017). It acts by catalyzing the oxidation of monophenols to diphenols, and subsequently to quinones. This process is followed by polymerization of quinones to melanin pigments (Larik et al., 2017). Melanins protect the skin from damage triggered by UV absorbed from sunlight and remove reactive oxygen species (ROS). However, overproduction of melanin leads to its accumulation in the skin causing dermatological conditions such as freckles, melasma, age spots, and melanoma (Haldys et al., 2018). More seriously, tyrosinase-catalyzed oxidation of dopamine to dopamine quinone derivatives is thought to be a key step in the etiology of Parkinson's disease (Anasuma et al., 2003; Hasegawa et al., 2003; Hasegawa 2010). Tyrosinase is also responsible for undesirable browning in vegetables and fruits, causing decrease in nutritional quality and economic loss. Thus, tyrosinase inhibitors may find applications in various fields, e.g. as cosmetics, as medication and in agriculture. (Gou et al., 2017; Si et al., 2012).

Previous work showed flavonols to be promising tyrosinase inhibitors (Şöhretoğlu et al., 2018b). Following this lead, we aimed to investigate tyrosinase inhibitory potential of some flavones possessing methoxy substitution (Fig. 1), and propose a mechanism of action based on *in vitro* enzyme kinetics and *in silico* molecular docking studies. Further, we assessed druglike properties of the most active two compounds using *in silico* methods.

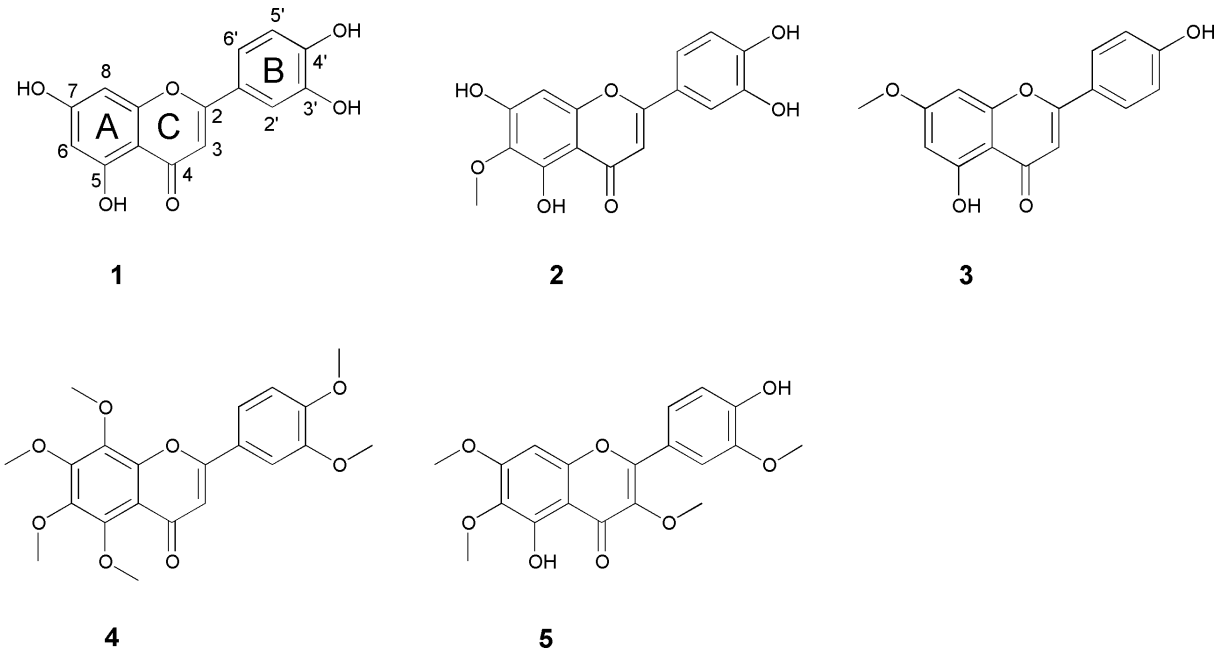

Figure 1*: Structures of the flavones* ***1*** *= Luteolin,* ***2*** *= Eupafolin (6-methoxyluteolin, nepetin),* ***3*** *= Genkwanin,* ***4*** *= Nobiletin,* ***5*** *= Chrysosplenetin*

2. EXPERIMENTAL

2.1 Materials

Kojic acid (KA), L-3,4-dihydroxyphenylalanine (L-DOPA), and mushroom tyrosinase (E.C. 1.14.18.1) were bought from Sigma-Aldrich (St. Louis, MO). All other chemicals used were analytical grade.

2.2 Tyrosinase inhibitory effects

The tyrosinase inhibition assay was done as described previously (Arslan et al., 2018). Kojic acid (KA) was used as positive control and methanol (1% v/v in 100 mM phosphate buffer, pH 6.8) as negative control. The reaction mixturescomprising 100 µL phosphate buffer (pH 6.8, 100 mM), 20 µL of tyrosinase (250 U/mL) and 20 µL tested compounds, were incubated for 10 min at room temperature. After preincubation, 20 µL L-DOPA (3 mM) was added in

the microplate and incubated for 10 min. The absorbance at 475 nm was measured using microplate reader (Thermo Scientific, Multiskan Go). The concentrations of the compounds that caused 50% tyrosinase inhibition (IC_{50}) were calculated using the following formula;

% inhibition: (C-A) / C × 100

Where C is the activity of the enzyme without compound and A is the activity of the enzyme in the presence of the compound.

2.3 Tyrosinase inhibition kinetic analysis

The kinetic analysis for the compounds was carried out to evaluate the inhibitory types and inhibitory constant (K_i) values using Lineweaver-Burk and Dixon plots (Lineweaver and Burk, 1934; Butterworth, 1972). The kinetic analysis was performed according to the inhibition assay detailed above.

2.4 Statistical analysis

All the data were analyzed by GraphPad Prism 5.0. The results were expressed as mean ± standard deviation (n=3). The differences among the compounds were investigated by one-way analysis of variance (ANOVA) followed by Tukey tests. $p < 0.0001$ was considered to be significant.

2.5 Molecular modelling

The compounds were modelled and optimized using MacroModel (2018-4, Schrödinger, LLC, New York, NY, 2018) and OPLS_2005 force field parameters (Banks 2005). LigPrep (2018-4, Schrödinger, LLC, New York, NY, 2018) was used to guess possible tautomeric and ionization states. The descriptors and properties of the ligands were calculated using QikProp (2018-4, Schrödinger, LLC, New York, NY, 2018). The crystal structural of mushroom

tyrosinase (PDB ID: 2Y9X (Ismaya 2011]) was downloaded from RCSB Protein Data Bank (www.rcsb.org) (Berman 2000) and prepared for docking with the Protein Preparation Wizard (2018-4, Schrödinger, LLC, NY, 2018) (Sastry 2013) of Maestro (2018-4, Schrödinger, LLC, NY, 2018). In this process, undesired residues were removed and the protons were treated with Epik (2018-4, Schrödinger, LLC, New York, NY, 2018), water orientations were sampled and H bonds were assigned by Propka. Receptor grid was generated for the catalytic site taking the centroid coordinates of the co-crystallized ligand, tropolone. Ligands were docked to this grid flexibly using Glide (2018-4, Schrödinger, LLC, New York, NY, 2018) at extra precision mode with 50 runs for each ligand (Friesner 2004, Halgren 2004, Friesner 2006). Docking scores are expressed as XP GScore in kcal/mol. Tropolone was re-docked to the receptor using Glide with above settings and its binding modes were close to their original conformations (RMSD: 1.33 Å).

3. RESULTS AND DISCUSSION

3.1 Inhibitory effects of the compounds on tyrosinase

The IC_{50} values of **1**-**5** are presented in Table 1. KA was used as positive control. Among the tested flavones, **5** showed the highest inhibitory effect on tyrosinase (IC_{50}: 99.87 ± 2.38 µM), even though it lacks the B-ring catechol moiety seen in compounds **1** and **2**, which is often associated with strong tyrosinase inhibition (Kim et al., 2006). The three strongest inhibitors in the current series all have methoxy substituents on the C-3' in the B-ring which, based on previous literature, would have been expected to reduce the inhibitory activity (Vaya et al., 2011). Also, presence of a methoxy group at C-6 on ring A, as seen in **2**, **4**, and **5,** does not reduce the inhibitory activity compared to flavones **1** and **2**, which is consistent with previously reported results where prenylation of C-6 did not affect tyrosinase inhibitory

activity (Zheng et al., 2009). If anything, the 6-methoxy group seems to enhance the tyrosine inhibitory activity since **2** showed much higher inhibition than **1** and the only difference between the two flavones is the additional methoxy group in the A-ring at C-6 in **2**.

In contrast, substitution of the C-7 hydroxy group by a methoxy dramatically decreases the inhibitory effect; flavone **3** had the highest IC_{50} of the tested compounds (281.60 ± 2.29 µM). This confirms the importance of the C-7 hydroxyl of flavonoids which has been reported before. Docking models suggested two alternative binding modes for polyhydroxy flavones, i.e. one where the 4'-hydroxyl faces the reactive centre in the tyrosinase and one where the 7-hydroxyl faces the copper ions in the enzyme (Kim et al., 2006; Şöhretoğlu et al., 2018b).

TABLE 1 Tyrosinase inhibitory effects of the flavones tested

Compound	**IC_{50} (µM)**
Luteolin (**1**)	265.30 ± 2.90*
Eupafolin (**2**)	209.21 ± 3.35*
Genkwanin (**3**)	281.60 ± 2.29*
Nobiletin (**4**)	131.92 ± 1.75*
Chrysosplenetin (**5**)	99.87 ± 2.38*
Kojic acid	50.00 ± 0.50

*$p < 0.0001$ (comparing to kojic acid)

Further docking studies indicated that the hydroxyl groups of B ring of luteolin interact with Asn81 and Cys83 of mushroom tyrosinase (Zhang et al. 2017). Small differences in the structures of compounds can cause significant differences on enzyme inhibitory properties. However, our data show that the substitution of hydroxyl groups by methoxy groups does not by default decrease the tyrosinase inhibitory action of flavones. The two strongest inhibitors in our assays are highly methoxylated compounds.

3.2 Kinetic analysis of tyrosinase inhibition

The modes of inhibition and K_i values of all the tested compounds on tyrosinase were determined by Lineweaver-Burk and Dixon plots (**Figs. 2** and **3)** and are summarized in **Table 2**.

TABLE 2 The results of kinetic studies of tested flavones on tyrosinase

Compound	**Type**	***K*i (μM)**
Luteolin (**1**)	Non-competitive	130.20 ± 0.22
Eupafolin (**2**)	Competitive	110.15 ± 0.25
Genkwanin (**3**)	Non-competitive	130.25 ± 0.53
Nobiletin (**4**)	Competitive	41.40 ± 0.42
Chrysosplenetin (**5**)	Competitive	14.10 ± 0.20

The Lineweaver-Burk plots of **2**, **4**, and **5** (Fig. 2) revealed that the K_m values increased with increasing inhibitor concentration and the V_{max} values remained the same, showing that these compounds inhibited tyrosinase via competitive manner, meaning that they may bind to the substrate binding site of tyrosinase (Barut et al., 2017). The K_i values of **2**, **4** and **5** were determined to be 110.15 ± 0.25, 41.40 ± 0.42 and 14.10 ± 0.20 μM, respectively (Fig. 3). In contrast, for **1** and **3** K_m values remained the same whilst V_{max} diminished with increasing concentrations of inhibitors and L-DOPA as the substrate (Fig. 2). The results represented that **1** and **3** were noncompetitive inhibitors that might interact with allosteric sites rather than with the catalytic site of the enzyme. The data were consistent with those reported previously (Zhang 2017; Lin et al., 2014; Bouzaiene et al., 2016; Zhang et al., 2007). The Dixon plots showed that the K_i values of **1** and **3** were 130.20 ± 0.22 and 130.25 ± 0.53 μM, respectively Fig. 3).

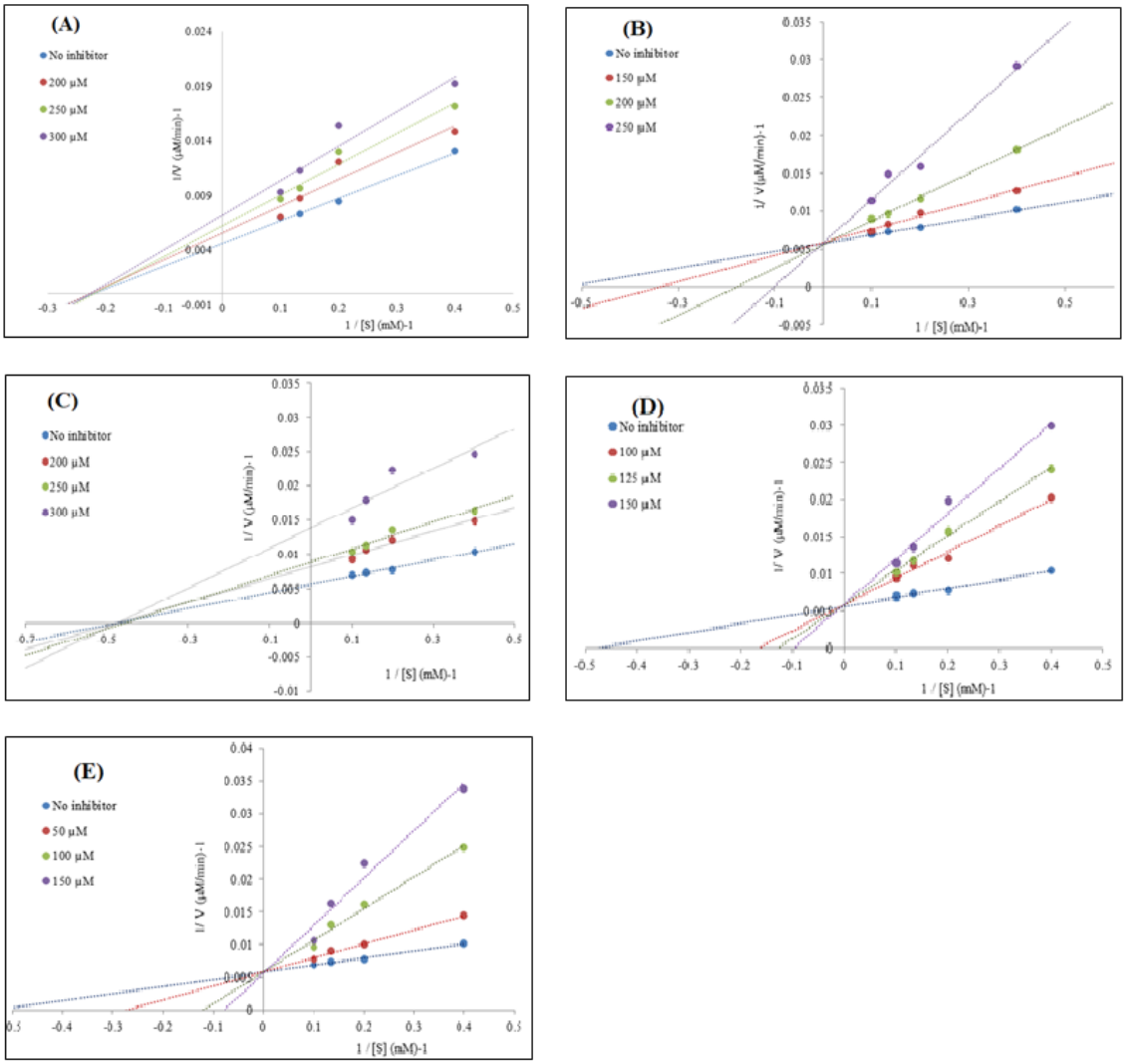

***Figure 2**: Lineweaver-Burk plots of the **1-5** against tyrosinase enzyme; (A) **1**, (B) **2**, (C) **3**, (D) **4** and (E) **5**.*

3.3 Druglikeness of of 4 and 5

QikProp software is designed to calculate a range of pharmaceutically relevant descriptors of **4** and **5** by comparison with those of the 95% of a dataset of known drug and druglike compounds. Especially descriptors such as molecular weight, hydrogen bond donor and acceptor counts, log*P*, number of rotatable bonds, and total polar surface area are considered as important parameters for druglikeness (Kelder 1999, Lipinski 2001, Mikitsh 2014).

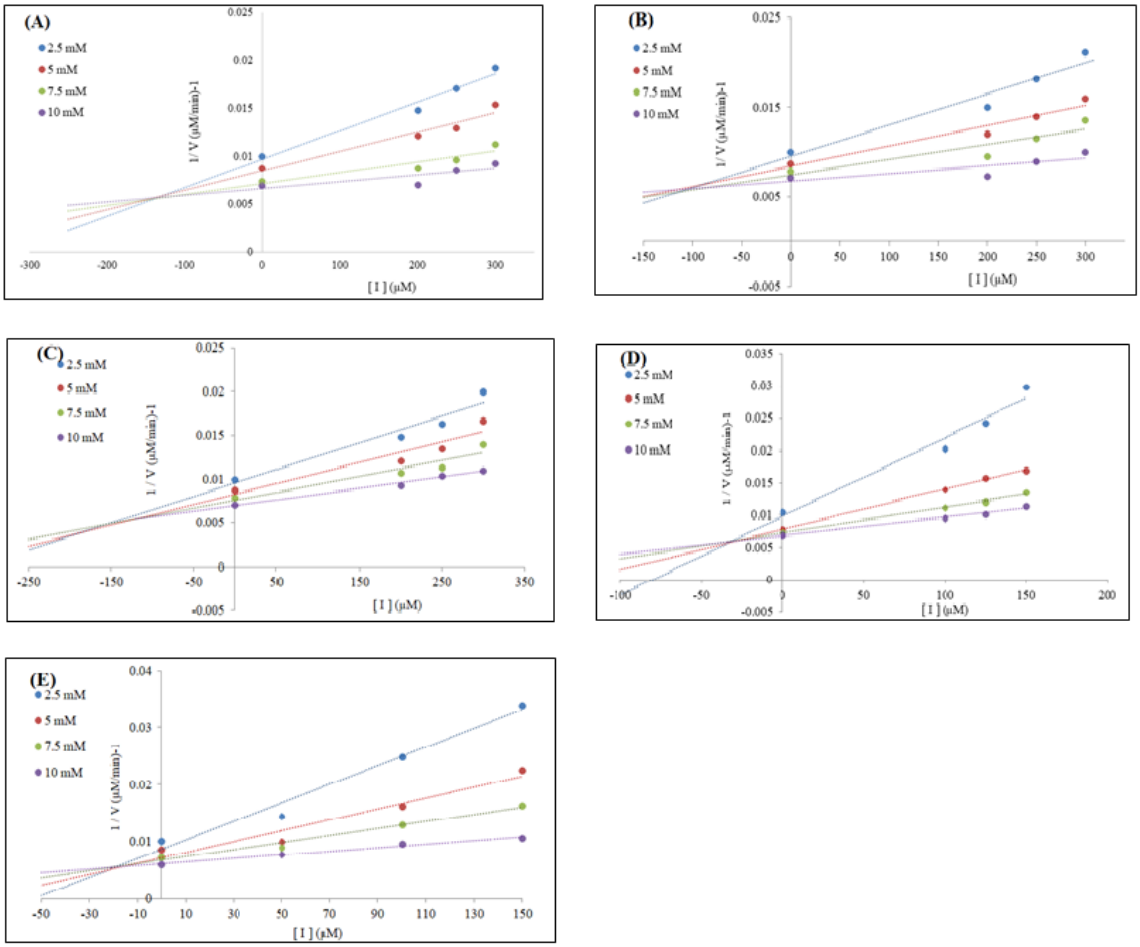

***Figure 3**: Dixon plots of the **1-5** against tyrosinase enzyme; (A) **1**, (B) **2**, (C) **3**, (D) **4** and (E) **5**.*

According to the predicted values, compounds **4** and **5** were expected to have good ADME (absorption, distribution, metabolism, and excretion) properties.

The QikProp software also allowed predictions on drug metabolism and pharmacokinetic properties of 4 and 5, based on comparison with those of the 95% of a dataset of known drug and druglike compounds (data not shown). Preliminary predictions indicate that descriptors of blood-brain barrier permeability were better for **4**, which means that **4** might cross to the central nervous system via passive diffusion at therapeutic concentrations.

3.4 Molecular docking to mushroom tyrosinase

Tyrosinases occur as tetramers comprising two pairs of identical subunits (H and L) (Strothkamp 1976). The catalytic subunit, H, includes a binuclear copper-binding site at the heart of four α-helices. The copper ions are coordinated with three histidine residues each (His61, His85, His94, and His259, His263, His296). These histidine residues interact with the nearby residues such as Phe90 and Phe292, thus possess limited side chain flexibility to maintain the copper-binding site stability (Hazes 1993, Ismaya 2011). His85 is also is covalently bound to Cys83 with a thioether bond through the side chain. Therefore, an effective and stable binding to tyrosinase catalytic site requires interactions with the coppers as well as their histidine ligands and other nearby residues (Ferro 2018), although a number of allosteric sites were previously suggested (Şöhretoğlu 2018a).

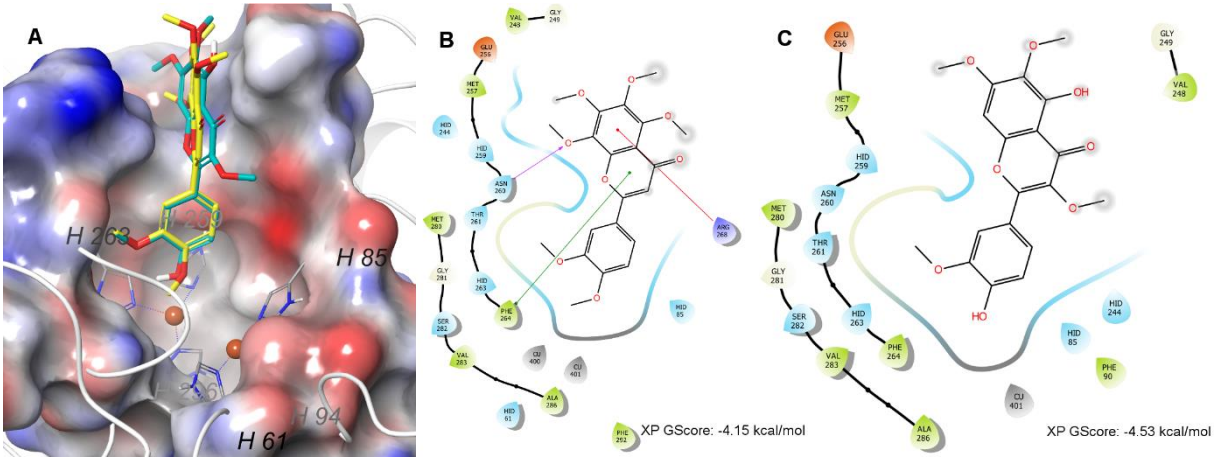

Figure 4*: The binding mode and interactions of* ***4*** *(A and B) and* ***5*** *(A and C).* ***4*** *is shown as yellow and* ***5*** *as blue sticks, copper ions as orange spheres, and the receptor as color molecular surface according to the electrostatic potential of the atoms. H bonds are showed as purple, π-π interactions as green, π-cation interactions as red lines.*

The docking poses of **4** and **5** in the catalytic site were very well superimposed with docking scores -4.15 and -4.53 kcal/mol, respectively. Compound **5** had a slightly higher predicted affinity for the active site than **4**. Both compared well to kojic acid (-4.80 kcal/mol) which we reported in our previous study (Şöhretoğlu 2018b). The 4'-methoxy oxygen of the B-ring of **4** and the 4'-hydroxy oxygen of the B-ring of **5** were located roughly 3 Å from one copper and 4.5 Å from the other copper fitting well in this cavity (Figure 4). The chromone rings of both ligands fit in the narrow neck between Val248 and Phe264 with the methoxy groups contacting the residues at the entry of the active gorge. The aromatic A-ring of the ligands failed to show key interactions with the nearby histidine residues although the chromone of **4** made π-π interactions with Phe264, π-cation interactions with Arg268, and H-bonded with Asn260. Rings B of both compounds were in hydrophobic contacts with His61, His85, and His263 while ring A H-bonded with His259 (Figure 4). These residues were reported as catalytic site residues (Ismaya 2011) and cited among other residues to interact with potential inhibitors (Şöhretoğlu et al., 2018b, Si et al. 2012, Wang et al. 2014, Zhang et al. 2017). The compounds showed good binding to the active site, but an alternative binding mode, in which the chromone ring would fit in the cavity near the bi-nuclear copper, was not possible due to the steric hindrance that would be caused by the bulky methoxy substitutions on the A-ring of this moiety.

Several flavones and flavonols with a catechol moiety in their B-ring have been shown to be competitive inhibitors of mushroom tyrosinase (Bouzaiene et al., 2016; Kim et al., 2006; Şöhretoğlu et al., 2018b; Vaya et al., 2011; Zhang et al., 2007; Zhang et al., 2017). Due to their structural resemblance, these compounds can displace L-DOPA and their catechol group then binds with the copper ions in the catalytic domain of tyrosinase (Kubo et al., 2004). In addition to being inhibitors, the flavone luteolin and the flavonol quercetin are also substrates for mushroom tyrosinase get converted into their respective *o*-quinones (Balyan et al., 2005;

Fenoll et al., 2003). The *o*-quinone products have altered pharmacological properties, e.g. luteolin *o*-quinone is an inhibitor of glutathione S-transferase and may be used to combat GST-induced drug resistance in melanomas (Awad et al., 2002; Balyan et al., 2005; Hayeshi et al., 2007). However, it is prudent to be cautious. Arguably, rather than inhibiting the formation of quinones, catechol-type flavones introduce new quinones into the mix, and the exact consequences are hard to predict. In contrast, methoxy flavones act as competitive inhibitors of tyrosinase, but are not substrates for the enzyme.

*TABLE 3 Predicted drug-like properties for compounds **4** and **5***

Descriptor	**4**	**5**	**Recommended range or values**
Rotatable bonds	6	6	0 to 15
Molecular weight (Da)	402.4	374.3	130 to 725
H-bond donor	0	1	0 to 6
H-bond acceptor	7	6	2 to 20
Log *P*	3.49	2.94	−2.0 to 6.5
Polar surface area ($Å^2$)	73.67	103.48	7 to 200

Whereas methoxy flavones do competitively inhibit tyrosinase, their application in cosmetic or medicinal products that aim to decrease tyrosine or dopamine oxidation should be treated with caution. Experiments with murine B16/F10 melanoma cells have shown that treatment with polyhydroxy flavones results in reduced melanogenesis (Horibe et al., 2013; Kumagai et al., 2011) but that polymethoxy flavones affect cell signaling, and induce tyrosinase expression and melanogenesis (Chung et al. 2017; Horibe et al., 2013; Kim et al., 2015b; Ko et al., 2014; Kumagai et al., 2011; Yoon et al., 2007, 2015a, 2015b). However, similar

experiments with human rather than murine melanocytes have shown that polymethoxy flavones inhibit the induction of melanogenesis (Kim et al. 2015a).

3.5 Conclusions

The polymethoxy flavones **4** (nobiletin) and **5** (chrysosplenetin) were the most potent tyrosinase inhibitors among the tested compounds, though overall the inhibitory activity of methoxylated flavones was only modest. Enzyme kinetics analyses revealed that **2** (eupafolin), **4**, and **5** were competitive tyrosinase inhibitors.

Molecular docking studies demonstrated that the most active compounds can bind to the catalytic site of tyrosinase with good affinity and interact with key residues, notably with copper ions, in the enzyme. In terms of druglikeness and pharmacokinetics (Hay 2014), modelling studies predicted that these flavones should be considered as promising candidates for further drug development.

4. REFERENCES

Arslan T, Keleş T, Barut B, Özel A, Biyiklioglu Z. Synthesis of novel monostyryl and distyryl boron dipyrromethenes bearing 4-((2-hydroxyethyl)(methyl)amino group as cholinesterase and tyrosinase inhibitors. Inorganica Chimica Acta 2018; 471: 121-125.

Asanuma M, Miyazaki I, Ogawa N. Dopamine- or L-DOPA-induced neurotoxicity: the role of dopamine quinone formation and tyrosinase in a model of Parkinson's disease. Neurotoxicity Research, 2003, Vol. 5 (3): 165-176

Awad HM, Boersma MG, Boeren S, van der Woude H, van Zanden J, van Bladeren PJ, Vervoort J, Rietjens IMCM. Identi¢cation of *o*-quinone/quinone methide metabolites of quercetin in a cellular in vitro system. FEBSLetters 2002, 520: 30-34

Banks L, Beard HS, Cao Y, Cho AE, Damm W, Farid R, Felts AK, Halgren TA, Mainz DT, Maple JR. Integrated modeling program, applied chemical theory (IMPACT), J. Comput. Chem. 2005; 26: 1752–1780.

Barut EN, Barut B, Engin S, Yıldırım S, Yaşar A, Türkiş S, Özel A, Sezen FS. Antioxidant capacity, anti-acetylcholinesterase activity and inhibitory effect on lipid peroxidation in mice brain homogenate of *Achillea millefolium*, Turkish Journal of Biochemistry 2017; 42(4): 493–502

Berman HM, Westbrook J, Feng Z, Gilliland G, Bhat TN, Weissig H, Shindyalov IN, Bourne PE. The protein data bank. Nucleic Acids Res. 2000; 28: 235–242.

Bouzaiene N, Chaabane F, Sassi A, Chekir-Ghedira L, Ghedira K. Effect of apigenin-7-glucoside, genkwanin and naringenin on tyrosinase activity and melanin synthesis in B16F10 melanoma cells, Life Sciences 2016; 144: 80-85.

Butterworth P. The use of Dixon plots to study enzyme inhibition, Biochimica et Biophysica Acta (BBA) – Enzymology 1972; 289: 251-253.

Chen J, Yu X, Huang Y. Inhibitory mechanism of glabridin on tyrosinase, Spectrochimica Acta Part A: Molecular and Biomolecular Spectroscopy 2016; 168: 111-117.

Chung YC, Kim S, Kim JH, Lee GS, Lee JN, Lee NH, Hyun CG. Pratol, an O-Methylated Flavone, Induces Melanogenesis in B16F10 Melanoma Cells via p-p38 and p-JNK Upregulation. Molecules 2017, 22: Article 1704

Ferro S, Deri B, Germanò MP, Gitto R, Ielo L, Buemi MR, Certo G, Vittorio S, Rapisarda A, Pazy Y, Fishman A, De Luca L. Targeting Tyrosinase: Development and Structural Insights of Novel Inhibitors Bearing Arylpiperidine and Arylpiperazine Fragments, J. Med. Chem. 2018; 61: 3908-3917.

Friesner RA, Banks JL, Murphy RB, Halgren TA, Klicic JJ, Mainz DT, Repasky MP, Knoll EH, Shaw DE, Shelley M, Perry JK, Francis P, Shenkin PS. A new approach for rapid,

335 accurate docking and scoring. 1. Method and assessment of docking accuracy, J. Med.
336 Chem. 2004; 47: 1739–1749.
337 Friesner RA, Murphy RB, Repasky MP, Frye LL, Greenwood JR, Halgren TA, Sanschagrin
338 PC, Mainz DT. Extra precision glide: docking and scoring incorporating a model of
339 hydrophobic enclosure for protein-ligand complexes, J. Med. Chem. 2006; 49: 6177–6196.
340 Gou L, Lee J, Hao H, Park Y, Zhan Y, Lü Z. The effect of oxaloacetic acid on tyrosinase
341 activity and structure: Integration of inhibition kinetics with docking simulation,
342 International Journal of Biological Macromolecules 2017; 101: 59-66.
343 Haldys K, Goldeman W, Jewginski, Wolinska E, Anger N, Rossawska J, Latajka R.
344 Inhibitory properties of aromatic thiosemicarbazone on mushroom tyrosinase: Synthesis,
345 kinetic studies, molecular docking and effectiveness in melanogenesis inhibition,
346 Bioorganic Chemistry 2018; 81: 577-586.
347 Halgren TA, Murphy RB, Friesner RA. Beard HS, Frye LL, Pollard WT, Banks JL. Glide: A
348 New Approach for Rapid, Accurate Docking and Scoring. 2. Enrichment Factors in
349 Database Screening, J. Med. Chem. 2004; 47: 1750–1759.
350 Hasegawa T, Matsuzaki M, Takeda A, Kikuchi A, Furukawa K, Shibahara S, Itoyama Y.
351 Increased dopamine and its metabolites in SH-SY5Y neuroblastoma cells that express
352 tyrosinase. Journal of Neurochemistry 2003, 87: 470–475
353 Hasegawa T. Tyrosinase-expressing neuronal cell line as in vitro model of Parkinson's
354 disease. Int. J. Mol. Sci. 2010, 11: 1082-1089
355 Hay M, Thomas DW, Craighead JL, Economides C, Rosenthal J. Clinical development
356 success rates for investigational drugs. Nature Biotechnol. 2014; 32: 40–51
357 Hayeshi R, Mutingwende I, Mavengere W, Masiyanise V, Mukanganyama S. The inhibition
358 of human glutathione S-transferases activity by plant polyphenolic compounds ellagic acid
359 and curcumin. Food and Chemical Toxicology 2007, 45: 286–295

Hazes B, Magnus KA, Bonaventura C, Bonaventura J, Dauter Z, Kalk KH, Hol WGJ. Crystal structure of deoxygenated *Limulus polyphemus* subunit II haemocyanin at 2.18 Å resolution: clues for a mechanism for allosteric regulation Protein Sci. 1993; 2: 597– 619.

Horibe I, Satoh Y, Shiota Y, Kumagai A, Horike N, Takemori H, Uesato S, Sugie S, Obata K, Kawahara H, Nagaoka Y. Induction of melanogenesis by 4'-*O*-methylated flavonoids in B16F10 melanoma cells. J. Nat. Med. 2013, 67(4): 705-710

Ismaya WT, Rozeboom HJ, Weijn A, Mes JJ, Fusetti F, Wichers HJ, Dijkstra BW. Crystal Structure of *Agaricus bisporus* Mushroom Tyrosinase: Identity of the Tetramer Subunits and Interaction with Tropolone. Biochemistry 2011; 50: 5477-5486.

Kelder J, Grootenhuis PD, Bayada DM, Delbressine LP, Ploemen JP. Polar molecular surface as a dominating determinant for oral absorption and brain penetration of drugs. Pharmaceutical Research 1999; 16(10): 1514-1519.

Kim D, Park J, Kim J, Han C, Yoon J, Kim N, Seo J, Lee C. Flavonoids as mushroom tyrosinase inhibitors: a fluorescence quenching study, J. Agric. Food Chem. 2006; 54: 935–941

Kim HJ, Yonezawa T, Teruya T, Woo JT, Cha BY. Nobiletin, a polymethoxy flavonoid, reduced endothelin-1 plus SCF-induced pigmentation in human melanocytes. Photochemistry and Photobiology 2015a, 91: 379–386

Kim HJ, Kim IS, Dong Y, Lee IS, Kim JS, Kim JS, Woo JT, Cha BY. Melanogenesis-inducing effect of cirsimaritin through increases in microphthalmia-associated transcription factor and tyrosinase expression. Int. J. Mol. Sci. 2015b, 16: 8772-8788

Ko HH, Chiang YC, Tsai MH, Liang CJ, Hsu LF, Li SY, Wang MC, Yen FL, Lee CW. Eupafolin, a skin whitening flavonoid isolated from *Phyla nodiflora*, downregulated melanogenesis: Role of MAPK and Akt pathways. Journal of Ethnopharmacology 2014, 151: 386-393

385 Kumagai A, Horike N, Satoh Y, Uebi T, Sasaki T, Itoh Y, Hirata Y, Uchio-Yamada K,
386 Kitagawa K, Uesato S, Kawahara H, Takemori H, Nagaoka Y. A potent inhibitor of SIK2,
387 3, 3', 7-trihydroxy-4'-methoxyflavon (4'-*O*-methylfisetin), promotes melanogenesis in
388 B16F10 melanoma cells. PLoS one 2011, 6(10): e26148
389 Larik FA, Saeed A, Channar PA, Muqadar U, Abbas Q, Hassan M, Seo S, Bolte M. Design,
390 synthesis, kinetic mechanism and molecular docking studies of novel 1-pentanoyl-3-
391 arythioureas as inhibitors of mushroom tyrosinase and free radical scavengers, European
392 Journal of Medicinal Chemistry 2017; 141: 273-281.
393 Lin F, Yen F, Chen P, Wang M, Lin C, Lee C, Ko H. HPLC-Fingerprints and antioxidant
394 constituents of *Phyla nodiflora*, The Scientific World Journal (2014); Article ID 528653.
395 Lineweaver H, Burk D. The determination of enzyme dissociation constants, Journal of The
396 American Society 1934; 56 (3): 658-666.
397 Lipinski CA, Lombardo F, Dominy BW, Feeney PJ. Experimental and computational
398 approaches to estimate solubility and permeability in drug discovery and development
399 settings. Advanced Drug Delivery Reviews 2001; 46(1-3): 3-26.
400 Mikitsh, JL, Chacko AM. Pathways for small molecule delivery to the central nervous system
401 across the blood-brain barrier. Perspectives in Medicinal Chemistry 2014; 6: 11-24.
402 Sastry GM, Adzhigirey M, Day T, Annabhimoju R, Sherman W. Protein and ligand
403 preparation: parameters, protocols, and influence on virtual screening enrichments, J.
404 Comput. Aid. Mol. Des. 2013; 27: 221–234.
405 Şöhretoğlu D, Sari S, Barut B, Özel A. Tyrosinase inhibition by a rare neolignan: Inhibition
406 kinetics and mechanistic insights through in vitro and in silico studies. Computational
407 Biology and Chemistry 2018a; 76: 61-66.

Şöhretoğlu D, Sari S, Barut B, Özel A. Tyrosinase inhibition by some flavonoids: Inhibitory activity, mechanism by in vitro and in silico studies. Bioorganic Chemistry 2018b; 81: 168-174.

Si YX, Wang ZJ, Park D, Chung HY, Wang SF, Yan L, Yang JM, Qian GY, Yin SJ, Park YD. Effect of hesperetin on tyrosinase: inhibition kinetics integrated computational simulation study, Int. J. Biol. Macromol. 2012; 50: 257-262.

Strothkamp KG, Jolley RL, Mason HS. Quaternary structure of mushroom tyrosinase. Biochemical and Biophysical Research Communications 1976; 70 (2): 519-24

Vaya J, Tavori H, Khatib S. Structure-activity relationships of flavonoids. Current Organic Chemistry 2011, 15: 2641-2657

Wang Y, Zhang G, Yan J, Gong D. Inhibitory effect of morin on tyrosinase: insights from spectroscopic and molecular docking studies. Food Chem. 2014; 163: 226-233.

Yoon HS, Lee SR, Ko HC, Choi SY, Park JG, Kim JK, Kim SJ. Involvement of extracellular signal-regulated kinase in nobiletin-induced melanogenesis in murine B16/F10 melanoma cells. Biosci. Biotechnol. Biochem. 2007, 71 (7): 1781–1784

Yoon HS, Ko HC, Kim SJ, Kim SS, Choi YH, An HJ, Lee NH, Hyun CG. Stimulatory effects of a 5,6,7,3’,4’-pentamethoxyflavone, sinensetin, on melanogenesis in B16/F10 murine melanoma cells. Lat. Am. J. Pharm. 2015a, 34 (6): 1087-1092

Yoon HS, Ko HC, Kim, SS, Park KJ, An HJ, Choi YH, Kim SJ, Lee NH, Hyun CG. Tangeretin triggers melanogenesis through the activation of melanogenic signaling proteins and sustained extracellular signal-regulated kinase in B16/F10 murine melanoma cells. Natural Product Communications 2015b, 10(3): 389-392

Zhang C, Lu Y, Tao L, Tao X, Su X, Wei D. Tyrosinase inhibitory effects and inhibition mechanisms of nobiletin and hesperidin from citrus peel crude extracts, Journal of Enzyme Inhibition and Medicinal Chemistry 2007; 22(1): 83–90.

Zhang L, Zhao X, Tao G, Chen J, Zheng Z. Investigating the inhibitory activity and mechanism differences between norartocarpetin and luteolin for tyrosinase. A combinatory kinetic study and computational simulation analysis. Food Chemistry 2017; 223: 40-48.

Zheng ZP, Cheng KW, Tsz-Kin To J, Li H, Wang M. Isolation of tyrosinase inhibitors from *Artocarpus heterophyllus* and use of its extract as antibrowning agent. Mol. Nutr. Food Res. 2008, 52: 1530 – 1538